Organic & Biomolecular Chemistry

ROYAL SOCIETY OF CHEMISTRY

REVIEW

Cite this: *Org. Biomol. Chem.*, 2021, **19**, 4622

L-Dopa in small peptides: an amazing functionality to form supramolecular materials

Demetra Giuri, Paolo Ravarino and Claudia Tomasini *

Received 26th February 2021,
Accepted 4th May 2021

DOI: 10.1039/d1ob00378j

rsc.li/obc

L-Dopa (3,4-dihydroxyphenylalanine) is a chiral amino acid generated *via* biosynthesis from L-tyrosine in plants and some animals. The presence of multiple interacting sites makes L-Dopa a multifunctional building block for the preparation of supramolecular materials. The possibility to form hydrogen bonds and the presence of the aromatic ring allow L-Dopa molecules to interact through a series of non-covalent interactions. The additional presence of the catechol moiety really makes this compound unique: not only does it have implications in the self-assembly process of Dopa itself and with other substrates, but also it highly increases the number of applications of the final material, since it works as an antioxidant, radical trapper, metal chelator, reducing agent and adhesive. L-Dopa and catechol containing derivatives have been extensively introduced inside both synthetic and natural polymers to obtain amazing functional materials. In this review we report the preparation of small peptides containing L-Dopa, focusing on the supramolecular materials that can be obtained with them, ranging from fibrils to fibres, gels, films and coatings, all having the different applications mentioned above and many others.

1. Introduction

L-Dopa (3,4-dihydroxyphenylalanine, abbreviated as Z) is a chiral amino acid that is involved in several biosynthetic pathways. It is a multifunctional building block that leads to the preparation of various materials. Before describing the formation of supramolecular materials obtained with this amino acid, we introduce here its preparation and its properties.

The biosynthesis of L-Dopa takes place in several organisms, spanning from plants to animals, mushrooms and bacteria. It involves tyrosinase, a copper-dependent enzyme, that shows two distinct activities, both involving molecular oxygen: cresolase (or monophenolase) that is responsible for the *ortho*-hydroxylation of tyrosine and catecholase (or diphenolase) that oxidises *o*-diphenols to *o*-quinones.[1]

Dipartimento di Chimica Giacomo Ciamician – Università di Bologna – Via Selmi, 2-40126 Bologna, Italy. E-mail: claudia.tomasini@unibo.it

Demetra Giuri

Demetra Giuri obtained her Bachelor's and Master's degree cum laude *in industrial chemistry from the Dipartimento di Chimica Industriale "Toso Montanari" of the Alma Mater Studiorum University of Bologna (Italy). She obtained her PhD in organic chemistry in 2020 under the supervision of Professor Claudia Tomasini from the Dipartimento di Chimica "Giacomo Ciamician", University of Bologna. She is presently a post-doctoral fellow in the same group. Her research interest focuses on the preparation of supramolecular gels starting from peptide-based low molecular weight gelators.*

Paolo Ravarino

Paolo Ravarino obtained his Bachelor's degree in chemistry from the University of Torino (Italy) and his Master's degree in chemistry from the "Dipartimento di Chimica Giacomo Ciamician" of the Alma Mater Studiorum University of Bologna (Italy) in 2019. He started his PhD thereafter under the guidance of Professor Claudia Tomasini in the same university. His research interests focus on the synthesis and characterisation of peptide-based materials, ranging from low molecular weight gels to foldamers.

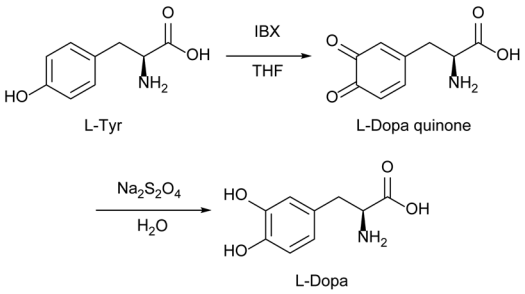

Fig. 1 The L-Dopa synthetic path followed by Bernini's group.

Mushroom tyrosinase is a widely used enzyme also for a synthetic approach due to its commercial availability and remarkable solubility.[2] Min *et al.* reported an example of an electroenzymatic reaction that reduces Dopa quinone *in situ* using a tyrosinase-immobilised cathode under the reduction potential of L-Dopa (−530 mV).[3] The high conversion rate obtained (95.9%) and the easy separation from the media make this methodology an interesting way to produce L-Dopa.

L-Dopa may be obtained also by chemical synthesis, using a chiral pool,[4] or by asymmetric catalysis.[5–8] These processes are often very long, use expensive catalysts or afford modest yields.

Based on a previous study on phenol oxidation,[9] another synthetic approach mimicking the activity of mushroom tyrosinase has been reported by Bernini *et al.* (Fig. 1).[10] They reported a one-pot synthesis of L-Dopa starting from L-Tyr and using 2-iodoxybenzoic acid (IBX) in a small excess for oxidation. It is worth noting that this process has a high yield (95%) and leaves the chiral centre unaltered.

L-Dopa is the precursor of dopamine, epinephrine and norepinephrine, which are neurotransmitters that play important roles in controlling health and well-being. Dopamine plays a central role in the treatment of Parkinson's disease, but is unable to cross the blood–brain barrier (BBB). For this reason, L-Dopa is used to increase dopamine levels in blood as it can cross the BBB.

Claudia Tomasini

Claudia Tomasini was born and educated in Bologna (Italy). She received her chemistry degree cum laude *in 1982 and her PhD in organic chemistry in 1986 from the Alma Mater Studiorum Università di Bologna (Italy). In 1987–1988, she was a postdoctoral associate at the University of Oxford, Oxford, UK. In 1990, she joined as assistant professor in the chemistry department of the Università di Bologna, where she is currently full professor. Her research interests include preparation and conformational studies of pseudopeptide foldamers and analysis of synthetic oligomers in solution and in the solid state for the formation of supramolecular materials.*

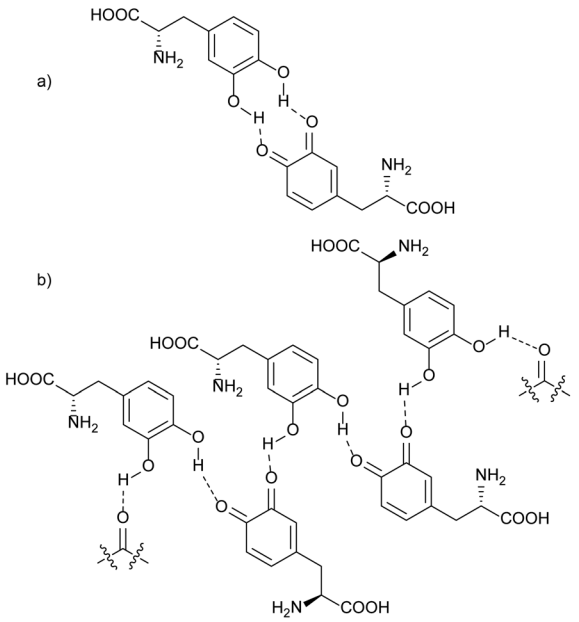

Fig. 2 Intermolecular hydrogen bonds between L-Dopa molecules in the reduced and oxidised forms: (a) bimolecular hydrogen bonds and (b) oligo- or polymolecular hydrogen bonds.

L-Dopa is also a crucial intermediate for the biosynthesis of several compounds: its oxidative polymerisation produces melanin and can be mimicked to prepare biomaterials such as eumelanin and pheomelanin.[11]

In addition, L-Dopa is present in naturally occurring polymers mainly synthesised by marine organisms,[12] such as *Mytilus edulis* (blue mussels) that secretes byssus.[13,14] It is a protein-based adhesive that is used by mussels to adhere to underwater surfaces, such as sea rocks and ship hulls, resisting even waves.[15,16] So far, roughly 25–30 different mussel foot proteins (mfp) have been identified in byssus.[14,15,17] Among them, mfp-3 and mfp-5 are probably the main mfp responsible for the adhesion to surfaces and they contain a particularly high amount (up to 30 mol%) of L-Dopa.[18] This effect suggests that this amino acid and in particular its catechol group have a dominant role in wet binding.[19]

The direct functionalization of polymers with Dopa and dopamine can be obtained through the formation of amide, urethane and ester linkages with the functional groups –NH_2, –COOH and –OH, as reported for synthetic polymers and biopolymers.[21]

Among the polymers functionalised with Dopa, wound sealants are noteworthy. They are biomaterials able to adhere to tissues by molecular cross-linking or through mechanical interlocking, acting as a glue.[28]

Synthetic materials tend to act as physical barriers, probably because of their lack of bioactivity for blood coagulation and wound healing. Fibrin-based sealants are the most

effective, but they are the most expensive and the risk of viral infections cannot be neglected. Other biopolymer-based materials are used, but none is really effective at stopping severe bleeding.[28] Wet adhesives with reduced complexity have been reported, consisting of low-molecular-weight catecholic zwitterionic surfactants, such as mussel foot proteins (mfp), which are polyelectrolytes with a high charge density.[27]

So far, several excellent reviews have been published on mussel-inspired polymers: hydrogels for biomedical[20–22] and environmental[23] applications, adhesives,[24,25] and antifouling coatings.[26] Many of them carefully describe the chemistry of the catechol group, the principles of wet adhesion with L-Dopa derivatives and the effect of oxidation, and the methods to prepare polymers containing L-Dopa, dopamine or catechol moieties.[20,21,25]

However, there are no reviews focusing on materials prepared with short peptides containing Dopa to the best of our knowledge. The aim of our review is to fill this gap with a journey through the small peptides based on L-Dopa, from single amino acids (like Fmoc-L-Dopa) to dipeptides and so on, slowly increasing the chain length. We will report self-assembled structures and the universe of applications that can be achieved using this simple building block.

We will present an overview of the materials that can be obtained, focusing on the formation techniques required to promote their self-assembly and on the properties of the material. For a better understanding, the examples will be organized, showing the materials that are formed by single protected L-Dopa, then by L-Dopa containing dipeptides, tripeptides, and so on until the use of hexapeptides. Finally, some examples of mfp analogues, containing up to 25 amino acids, will be reported.

2. Supramolecular materials obtained with short peptides containing L-Dopa

Molecular assembly is a ubiquitous process in nature. Peptides and proteins, for example, interact and self-organize to form well-defined structures associated with specific functionalities. Mimicking nature, we can exploit self-assembly for the preparation of an entirely novel class of synthetic materials.

The self-assembly of small molecules relies on weak non-covalent interactions, such as hydrogen bonds, electrostatic interactions, hydrophobic interactions and van der Waals interactions.[29,30]

Although very weak if isolated, these interactions gain significant importance when combined as a whole and are able to govern the formation of complex structures.[31]

Since one usual consequence of the self-assembly of small molecules, and in particular of peptides, is the formation of a gel (gelation), a subset of these compounds is that of low molecular weight gelators (LMWGs), which have gained increasing relevance in the last two decades.

Compared to their polymeric analogues, in which the random network is held together by strong covalent interactions and cross-linking, LMWGs rely on weak bonds and molecular assembly, thus making the process not only more ordered but also reversible.

It is possible to trigger the formation of a material under specific conditions and, in the same way, to induce the disassembly of the network if the conditions are reversed. For their ability to respond to external stimuli, LMWGs are considered a class of smart materials.

Sol–gel transition is usually induced by a stimulus (trigger), which can be physical (a temperature change, ultrasound, ionic strength modulation) or chemical (pH change, chemical or photochemical reactions, enzymes and catalysis).[32] The general method of preparation relies first on the dissolution of the gelator molecule in a solvent (water for hydrogels, organic solvent for organogels), followed by the addition of the trigger to the solution. This leads to the start of the assembly process, inducing the molecules to organise into supramolecular structures, which are usually fibres, that entangle together over time, resulting in a network able to entrap the solvent.

This class of soft materials is particularly interesting for several reasons; the first is the possibility to easily tune and control the chemical structure of the gelator and the conditions of the gelation process, thus changing the specific properties and applications of the final material. Moreover, LMWGs derived from amino acids and peptides are even more appealing thanks to their intrinsic biocompatibility and biological activity.[33]

L-Dopa is an ideal ligand for several substrates. The two hydroxyl groups form hydrogen bonds and their *ortho*-position makes L-Dopa a strong chelating agent, while the aromatic feature leads to π–π stacking, cation–π and van der Waals interactions. Nevertheless, the oxidised form, Dopa-quinone, is noteworthy: the two carbonyl groups can act as Lewis bases, even though weaker than the deprotonated catecholic form. The conjugated system of four double bonds enables the molecule to absorb and emit visible light. The quinone is also able to a hydrogen bond with the catechol (Fig. 2). The formation of these weak interactions is of remarkable importance when considering the preparation of an L-Dopa-based material: the cohesion strength is enhanced and so are the rheological properties.

We believe that the possibility to exploit Dopa and its functionalities as building blocks in supramolecular assembly is worth reporting since it leads to the preparation of amazing materials, with a wide range of architectures, properties, morphologies and applications.

2.1. Protected L-Dopa: a single amino acid gelator

Saha *et al.* were the first group to report a self-assembly study on a single amino acid gelator based on L-Dopa. The behaviour of Fmoc-L-Dopa solutions (0.5 wt%) in water was investigated under different pH conditions: pH = 2, 5, and 7.[34] Only at pH 2 was it possible to obtain a mechanically weak gel, while on increasing the pH, no gel was formed and the solutions turned brown in colour with time due to the oxidation of the catechol moiety. The characterisation of the solutions (CD, DLS, SAXS,

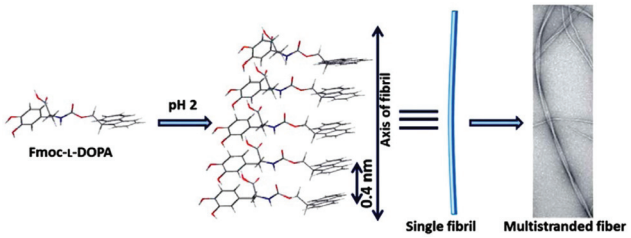

Fig. 3 Schematic representation of the proposed model of self-assembly of Fmoc-L-Dopa at pH 2. Adapted with permission from ref. 34. Copyright (2013) Royal Society of Chemistry.

TEM and cryo-TEM) allowed them to predict a schematic model for the self-assembly of Fmoc-L-Dopa at pH 2 (Fig. 3).

They proposed that monomers stack linearly along the axis of the fibril, stabilized *via* π–π interactions among the Fmoc groups. The possibility of intermolecular H-bonding between the C═O and N–H bonds of the adjacent carbamate groups was also proposed. This effect is favoured only at low pH, where the acidic moieties are protonated. In contrast, when the pH increases above 5, the carboxylic groups are deprotonated so that the Fmoc-L-Dopa molecules are ionized and this results in inhibition of fibril formation.

The assembly of Fmoc-L-Dopa (1 mg mL^{-1}) was also investigated in ethanol/water mixed solutions.[35] This solvent change method consists of the dissolution of the gelator in an organic solvent and the subsequent addition of a miscible anti-solvent, such as water, which reduces the solubility of the compound and induces the gelation process. Gazit *et al.* reported that, despite its apparent simplicity, under these conditions, Fmoc-L-Dopa participates in complex, spontaneous structural transitions with intermediate metastable assemblies. Upon the initiation of assembly, Fmoc-L-Dopa rearranges into metastable spheres, which are in continuous equilibrium with the dissolved monomers. The monomers serve as a reservoir for the formation of supramolecular assembly in the gel phase, mainly mediated by hydrophobic interactions. The disordered aspects of the spheres and the fibrillar assemblies arise from the interaction with solvent molecules. The conclusion of the transition process resulted in the formation of crystals, one month after the start of the process, producing a thermodynamically favourable ultrastructure. As reported in other works, the molecular packing of the gel phase is different from that observed in the crystal phase.[36] The Fmoc-Dopa system is considered a minimal model for the formation of supramolecular polymers (Fig. 4).

Later on, Gazit *et al.* investigated the behaviour of Fmoc-Dopa in a mixture of DMSO and water and in combination with Fmoc-Tyr.[37] In their work they demonstrated how the functionalities of Dopa can be exploited in multicomponent gels and are crucial to provide specific properties and achieve materials with interesting applications. When prepared from DMSO/water solutions (5 and 6.67 mg mL^{-1}), Fmoc-Dopa preparations were viscous and presented a weak, non-self-supporting gel-like behaviour, while Fmoc-Tyr hydrogels exhibited self-supporting gel characteristics within minutes after triggering.

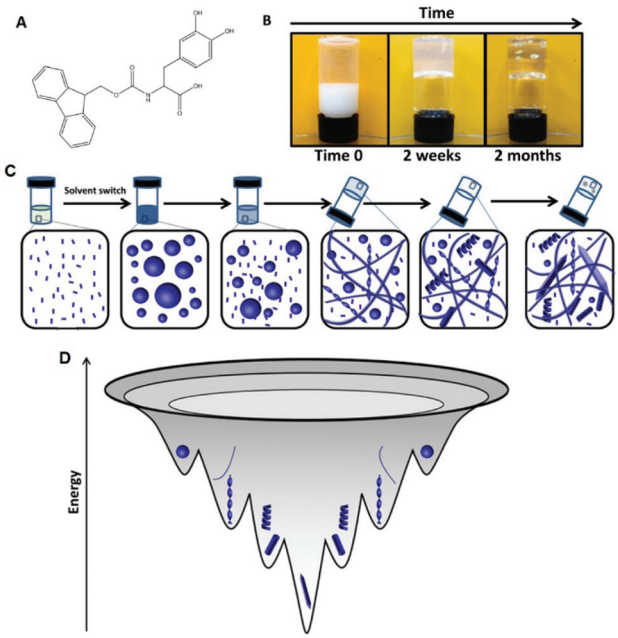

Fig. 4 (A) Chemical structure of Fmoc-L-Dopa. (B) Macroscopically observable changes of Fmoc-Dopa preparation over time. (C) Suggested model for the formation of supramolecular polymers based on Fmoc-Dopa, both at the macroscopic level and at the microscopic level. (D) Energy landscape of the Fmoc-Dopa transition process.

The mixed system combined the properties of the two components, joining the physical characteristics of Fmoc-Tyr gels and the functionality of the catechol groups of Dopa. The ability of the multicomponent hydrogel to reduce ionic silver to Ag nanoparticles (AgNP) was investigated. Silver nitrate solution was added to hydrogels which were then incubated for five days both in the presence and in the absence of ambient light. AgNP were detected in the Fmoc-Dopa and hybrid gel samples, as imaged by TEM (Fig. 5) and attributed to the catechol functionality and the presence of light.

An efficient way to obtain strong hydrogels (G' = 25–64 kPa depending on the trigger) with a single amino acid gelator based on L-Dopa was recently reported by Tomasini *et al.* with the synthesis of Boc-L-Dopa$(Bn)_2$-OH,[38] which is a Dopa derivative where the benzyl ethers linked to the catechol moiety proved to be essential for the formation of strong supramolecular gels, thanks to the additional π–π stacking interactions provided. The gels were prepared using two methods: pH change, using glucono-δ-lactone (GdL) as the trigger, and addition of $CaCl_2$, a divalent cation. The two methods led to the formation of materials with different mechanical properties, morphologies and structures. The gels prepared with $CaCl_2$ were used for the controlled growth of $CaCO_3$ crystals. The hydrogel represents a model for biomineralization studies as it behaves as an insoluble matrix that confines the calcification site, thus preserving its structure (Fig. 6) after the formation of the mineral phase.

Lee *et al.* reported the preparation of Dopa-C7 bolaamphiphile, composed of a central heptyl chain and two Dopa moi-

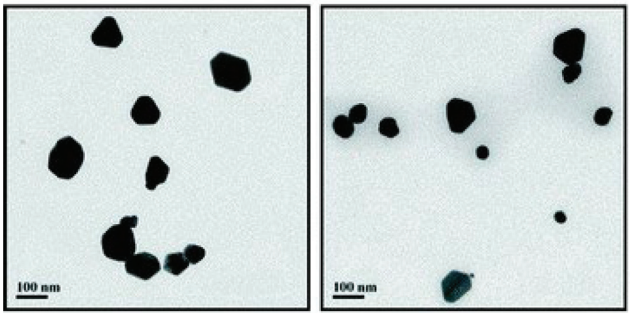

Fig. 5 TEM micrographs of silver nanoparticles detected in the samples of 1.67 mg mL^{-1} Fmoc-Dopa (left panel) and Fmoc-Tyr : Fmoc-Dopa 3 : 1 hybrid gels at 6.67 mg mL^{-1} (right panel), following incubation with silver nitrate in the presence of light. Adapted with permission from ref. 37. Copyright (2015) Royal Society of Chemistry.

eties at the ends (Fig. 7).[39] The self-assembly of the compound was used as a template to produce magnetic metal oxide core–shell nanoparticles. As the catechol group chelates the metal cations with its hydroxyl and quinone moieties, cobalt and iron ions were bound and subsequently reduced to form solid metal oxides on the Dopa-C7 self-assembly template.

Being an organic substance, the Dopa-C7 self-assembly does not show any magnetic susceptibility to an external magnetic field. In contrast, after deposition of a cobalt oxide or iron oxide layer, the core–shell particle shows linear magnetization over the external magnetic field with negligible coercivity and magnetic remanence. Cobalt oxide showed stronger magnetization than iron oxide.

The self-assembly of this compound is robust and stable even under vacuum and under dry conditions, with the adhesive properties arising from the surface-exposed catechols. The authors observed that when Dopa-C7 molecules are dissolved in aqueous solutions, they spontaneously self-assemble, creating nanospherical aggregates with exposed Dopa catechol moieties on the surface, which over time also aggregate forming bigger structures. These clusters then assemble through the hydrogen bond working between the dihydroxyphenyl groups to form spherical assembled structures (87.5 ± 9.1 nm in diameter).

This suspension was applied as an adhesive to modify the surfaces of various substrates. Dopa-C7 assemblies were stamped on a silicon wafer, leading to the formation of a coating on the surface (Fig. 8), with homogeneity higher than that of polydopamine.

Dopa-C7 assemblies also showed considerable adhesivity, originating from the hydrogen bonding of catechol groups,

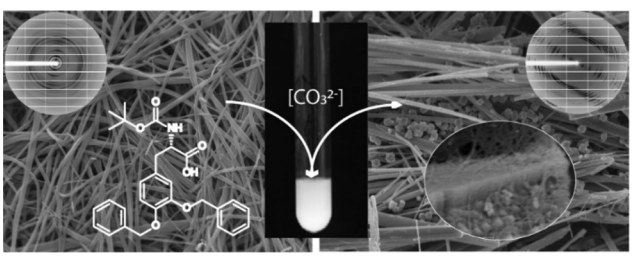

Fig. 6 Schematic depiction of the formation of Boc-L-Dopa(Bn)$_2$-OH hydrogels using two triggers, GdL and $CaCl_2$. Adapted with permission from ref. 38. Copyright (2019) American Chemical Society.

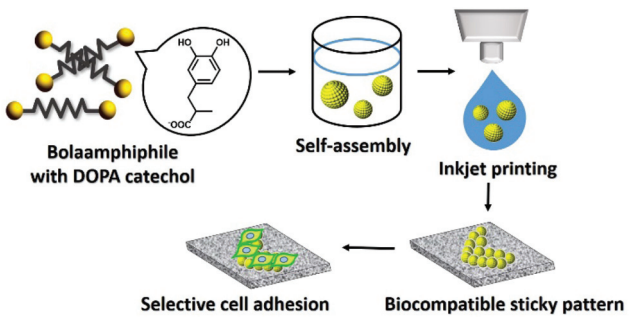

Fig. 8 Schematic illustration of the selective cell adhesion on a patterned surface that was prepared by inkjet printing of bolaamphiphile assemblies.

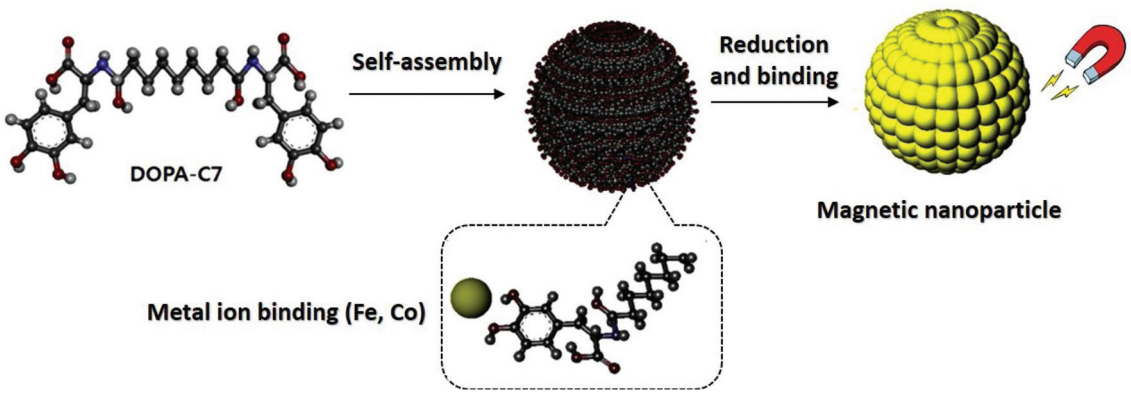

Fig. 7 Schematic layout of the Dopa-C7 self-assembly and subsequent metal ion adsorption for the synthesis of magnetic cobalt and iron oxide nanoparticles.

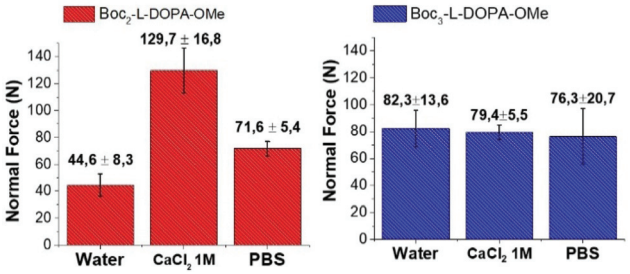

Fig. 9 Results for the traction tests of Boc_2-L-Dopa-OMe and Boc_3-L-Dopa-OMe.

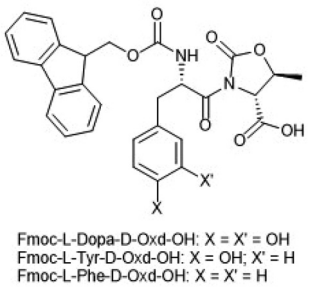

Fig. 10 Chemical structure of the gelators described.

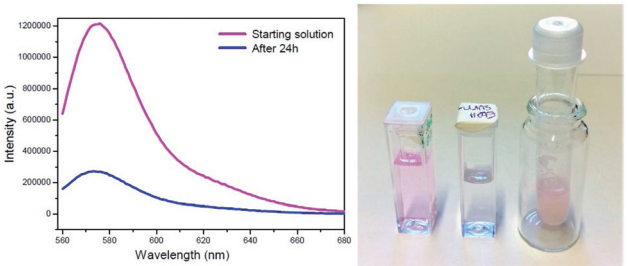

Fig. 11 (Left) Emission spectra of an aqueous solution of RhB (2.0 μM) before (pink) and after (blue) the treatment with the ethanol organogel for 24 hours. (Right) Photograph of an aqueous solution of the RhB sample before (left) and after (right) the treatment with the ethanol organogel, and the same organogel after the treatment.

remarkable enhanced cell adhesion, increased cell viability and lower toxicity compared to the other catechol-modified surfaces.

Tomasini *et al.* recently described a new class of Dopa-based adhesives that consists of extremely simple molecules,[40] where the catechol moiety is partly or fully protected with Boc groups.

Three molecules were synthesised to probe how the introduction of hydrophobic groups would affect the adhesive ability of the Dopa skeleton: Boc-L-Dopa-OMe, an inseparable mixture of *m*-Boc_2-L-Dopa-OMe and *p*-Boc_2-L-Dopa-OMe, and Boc_3-L-Dopa-OMe.

Three films were prepared by casting the molecules on a Petri dish. After solvent evaporation, the films became completely non-adhesive in the dry phase, while the adhesion was triggered after wetting with three aqueous media (H_2O, 1 M aqueous $CaCl_2$ and PBS at pH 7.4). In contrast, Boc-L-Dopa-OMe showed no adhesion capability either under dry or wet conditions.

The inseparable mixture of *m*-Boc_2-L-Dopa-OMe and *p*-Boc_2-L-Dopa-OMe registered an adhesive force up to 130 N in 1 M aqueous $CaCl_2$ (Fig. 9). In contrast, the adhesion registered with Boc_3-L-Dopa-OMe showed the best performances in other aqueous solutions suggesting that, even though the protection on the catechol prohibits cation chelation, it allows fast dehydration of the surface to bind.

2.2. Self-assembled L-Dopa containing di- and tri-peptides

After the first group of molecules containing a single L-Dopa unit, we report here the preparation of supramolecular materials based on longer peptides containing L-Dopa.

Tomasini *et al.* reported the gelation ability of Fmoc-L-Dopa-D-Oxd-OH, Fmoc-L-Tyr-D-Oxd-OH and Fmoc-L-Phe-D-Oxd-OH in water using several gelators (Fig. 10).[41]

They introduced the 4-methyl-5-carboxyoxazolidin-2-one (Oxd) moiety that is a derivative of threonine. This heterocycle introduces a constraint imposed by the *trans* conformation of the two adjacent carbonyls, which can favour the formation of fibre-like materials organized either in β-sheets or in supramolecular helices when combined with other factors like π-stacking interactions and intermolecular hydrogen bonds.[42] Indeed, when Oxd was replaced with Pro, only liquids or amorphous solids were obtained.

Supramolecular gels were prepared using these three gelators and ten different triggers. Hydrogel formation is very sensitive to the trigger and to the number of the hydroxyl moieties linked to the aromatic rings. The best triggers for these systems were GdL, $CaCl_2$ and $ZnCl_2$ leading to hydrogels with mechanical properties depending on the gelator used. Fmoc-L-Tyr-D-Oxd-OH was the strongest in all cases.

In a following work, Tomasini *et al.* reported a comparison between the gelation ability of Fmoc-L-Dopa$(Bn)_2$-D-Oxd-OBn and Lau-L-Dopa$(Bn)_2$-D-Oxd-OBn in several organic solvents using ultrasound sonication as the trigger. The first gelator was not able to form gels in any of the solvents.[43] The second one formed gels in toluene, ethyl acetate, acetonitrile, ethanol and methanol, suggesting that the presence of the saturated long chain of lauric acid was essential for its tendency to stick together producing fibres and micelles. The mechanical properties and melting point of the materials were found to be directly correlated to the polarity of the solvent, resulting in increasing strength moving from toluene to ethanol. The ethanol organogel was used to test the absorption of rhodamine B as a model pollutant from water. After 24 h, only 23% of the pollutant remained in the aqueous solution (Fig. 11).

Gazit *et al.* reported that L-Dopa-L-Dopa and Fmoc-L-Dopa-L-Dopa dipeptides were able to self-assemble into ordered nanostructures in the presence of ethanol and water.[44]

They observed the temperature-dependent formation of a gel for Fmoc-L-Dopa-L-Dopa (Fig. 12).

The authors investigated the redox properties of the assemblies containing the catechol moieties by monitoring the

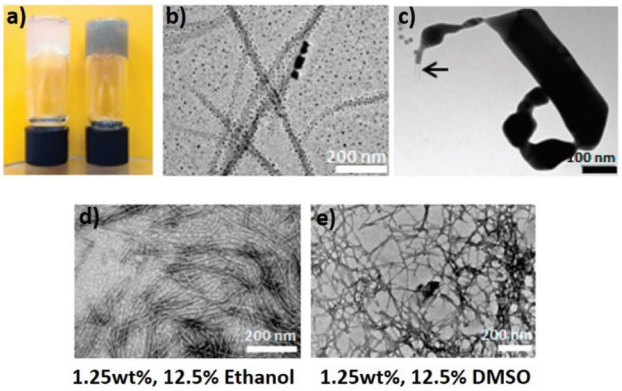

Fig. 12 (Top) (a) Macroscopic visualization of assemblies at 5 mg mL^{-1} taken after 5 days of incubation. (b) TEM micrographs of the formation of silver particles after 1 day of incubation of assemblies at 2.5 mg mL^{-1}. (c) TEM micrographs of the assemblies at 5 mg mL^{-1} after 3 days of incubation. The arrows indicate noncoated peptide assemblies (negative staining was not applied). (Bottom) TEM analysis of 1.25 wt% (17.2 mM) Fmoc-Dopa-Dopa-Lys assemblies prepared in either 12.5% ethanol (d) or 12.5% DMSO (e).

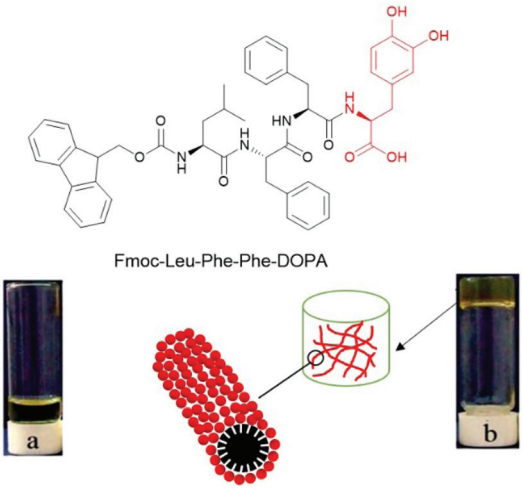

Fig. 13 Chemical structures of the hydrogelator (Fmoc-Leu-Phe-Phe-Dopa); (a) solution containing 40 mM of the starting materials with inactive metalloprotease, pH 7.4; (b) gel formed with the catalysis of metalloprotease after 5 min.

reduction of ionic silver. Although these assemblies possess redox activity, no adhesive properties were macroscopically observable. Therefore, they designed the Fmoc-L-Dopa-L-Dopa-L-Lys protected tripeptide, inspired by mussel foot proteins (mfp), which base their adhesive strength on the synergy between Dopa and Lys.

Under both ethanol and DMSO conditions, they observed that this tripeptide forms a viscoelastic glue capable of adhering two glass slides. In the presence of DMSO, the adhesive properties (more than 300 nN with AFM) showed recovery behaviour: after separating the glass slides by peeling, they were able to be rejoined, and AFM analysis revealed the presence of twisted spheres that were unidirectionally retracted. Interestingly, this did not happen in ethanol, where the adhesive force was also a bit lower (214 nN) and AFM analysis after peeling exhibited unidirectional fine fibrous structures. The authors therefore hypothesised that the existence of larger patches of peptide assemblies have a role in the re-adhesion process.

2.3. Self-assembled Dopa tetra- and pentapeptides

Materials obtained by the self-assembly of peptides containing 4 or 5 amino acids show interesting properties. In several examples described here, the property is exhibited by only one Dopa unit.

Xu *et al.* reported the preparation of a bioadhesive supramolecular hydrogel containing Dopa (Fmoc-Leu-Phe-Phe-Dopa) *via* protease catalysis (Fig. 13).[60]

As previously observed, the catechol groups are important for tuning the balance between hydrophilicity and hydrophobicity, thus affecting the molecule gelation behaviour. Then the ability of the gelators to promote *in vitro* cell adhesion and proliferation was evaluated. A hydrogel based on Fmoc-Lys-Phe-Phe without Dopa was used as the control. Adult human dermal fibroblast cells were seeded on top of the gels. The results showed that more cells adhered to the Dopa-containing gel, and cell viability (Fig. 14) at day 3 was 152% greater than at day 1 (35% more than the control). This result demonstrated that the unoxidized catechol groups are crucial to successfully promote the adhesion and proliferation of fibroblast cells, in comparison with gels that do not contain Dopa.

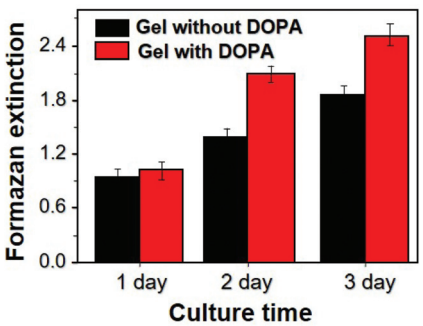

Fig. 14 Proliferation rate of cells on gels containing DOPA groups and the control (without DOPA) determined using the WST-8 method.

The peptide described by Li *et al.* is prepared through a different approach, by *in situ* enzymatic formation of Dopa hydrogels (5 mg mL^{-1}), using a simple reaction by tyrosinase[45] (Fig. 15). 2-Nap-Gly-Phe-Phe-Tyr (2Nap-GFFY) was used as the hydrogelator precursor. The hydrogel was formed in the presence of various amounts of silica nanospheres using the ENAC method (enzyme-assisted nanoparticle crosslinking). This method is inspired by the previously reported structure of marine mussel foot byssus.

After the hydrogel is formed, mushroom tyrosinase is added to convert the tyrosine residue into Dopa. As the cross-

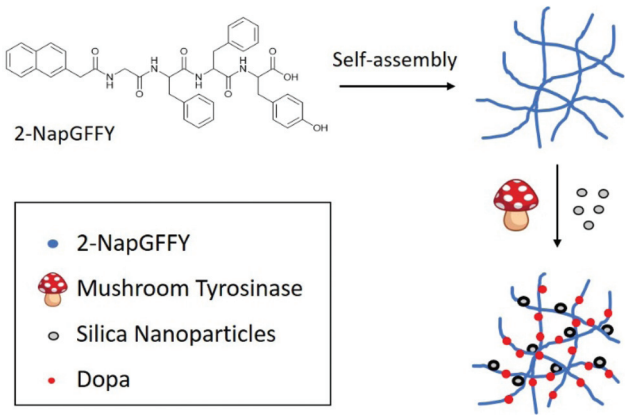

Fig. 15 Schematic illustration of the ENAC strategy for hydrogelation of 2-NapGFFY.

linking is introduced after the self-assembly of peptide fibrils, the interference between the two processes of fibril formation and of interactions between fibrils and silica nanoparticles is strongly reduced. Moreover, following this procedure, the mechanical stability of the hydrogel was significantly enhanced.

Gazit *et al.* reported the synthesis and the assembly into fibrillar structures of Asp-Dopa-Asn-Lys-Dopa, which is a pentapeptide containing two Dopa units.[46] The peptide was dissolved in water and sonicated for 10 min, leading to a viscous turbid solution for all the concentrations tested (100 μM to 15 mM). TEM analyses revealed a network of fibrillar assemblies, mostly linear, unbranched and extending to the length of micrometers (Fig. 16).

The CD and FTIR analysis suggested that Asp-Dopa-Asn-Lys-Dopa adopts in water either a random coil conformation or a β-turn conformation and that the β-turn structures self-assemble into supramolecular β-sheets, producing amyloid-like fibrillar assemblies.

Finally, the authors tested the ability of the peptide to reduce ionic silver, which was confirmed by the appearance of dark nanometric clusters on the fibrillar assemblies by both TEM and SEM. The clusters were not observed in a control solution to which $AgNO_3$ was not added (Fig. 16), while they seemed to have selectively deposited on the assemblies compared to the background. These results showed that Asp-Dopa-Asn-Lys-Dopa assemblies can reduce ionic silver while retaining their ultrastructure in solution.

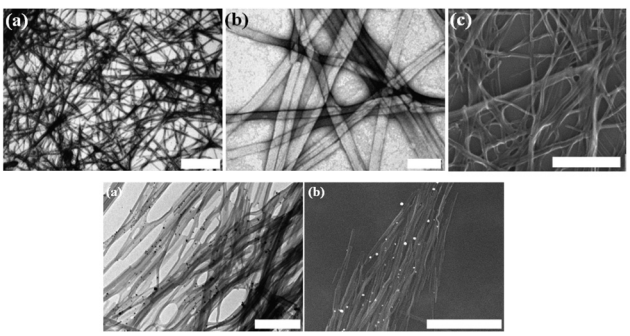

Fig. 16 (Top) High-resolution microscopy of fibrillar assemblies formed by 6 mM Asp-Dopa-Asn-Lys-Dopa in water. (a and b) Transmission electron microscopy (TEM) micrographs, negative staining was applied, scale bars represent 2 μm and 100 nm; (c) scanning electron microscopy (SEM) micrograph, scale bar represents 1 μm. (Bottom) Silver reduction by the Asp-Dopa-Asn-Lys-Dopa fibrillar assemblies. (a) TEM micrograph, negative staining was not applied, scale bar represents 500 nm; (b) respective SEM micrograph, metallic coating by sputtering was not applied. Scale bar represents 2 μm.

2.4 Self-assembled longer Dopa-containing chains

Longer peptides, containing one or more Dopa units deserve some attention, as they exhibit interesting properties.

Veldkamp *et al.* reported the incorporation of L-Dopa inside a series of peptides designed to adopt a β-hairpin configuration. They demonstrated that these peptides including L-Dopa were able to form metal:peptide complexes with zinc.[47]

Absorption spectroscopy has proven to be a useful technique in studying metal–catecholic interactions as the combination of these peptides and zinc gives rise to a spectrophotometric change. While neither the L-Dopa containing peptides nor zinc solutions have significant absorbance above 300 nm, the titration of zinc leads to an enhancement of the π–π* transition with red shifting and new absorbance between 300 and 350 nm appears with increasing zinc amount (Fig. 17).[48]

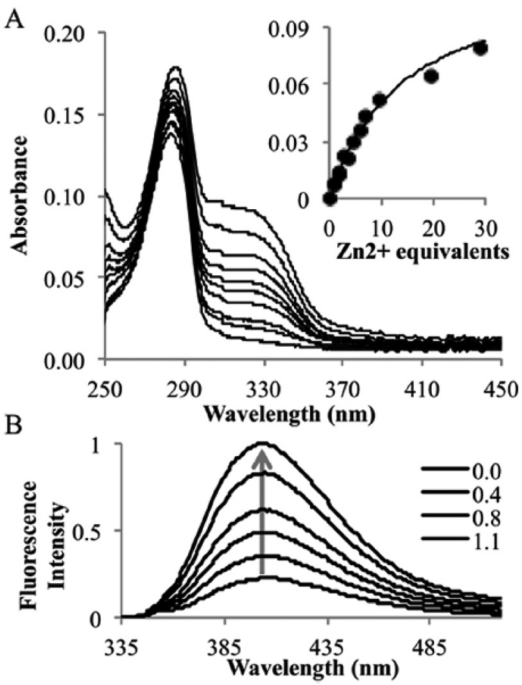

Fig. 17 (A) Spectrophotometric titration of DopaGly with Zn^{2+}; the inset shows the absorbance at 325 nm. (B) Fluorescence emission with zinc addition from 0 to 1.4 equivalents. Adapted with permission from ref. 47. Copyright (2017) Elsevier.

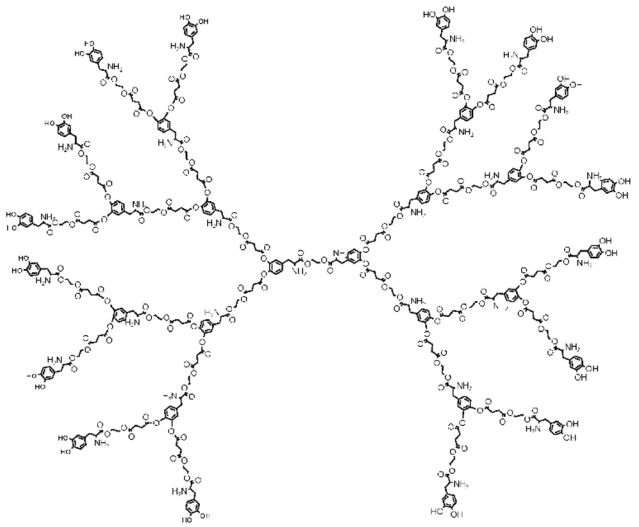

Fig. 18 Structure of the second-generation L-Dopa dendrimer prodrug (HO-G2-NH_2). Adapted with permission from ref. 49. Copyright (2006) American Chemical Society.

When the investigated DopaXxx peptides are mixed with zinc solutions, they all develop similar absorbance bands between 300–370 nm and experience a mild π–π* enhancement with modest changes to the k_{max} value between 278 and 283 nm.

Tang *et al.* reported the preparation of dendrimers (up to 30 residues) entirely made of L-Dopa (Fig. 18).[49] Their monodisperse nature was shown by NMR, MALDI-TOF-MS, and PAGE. The L-Dopa moieties were connected in the dendrimer to one another *via* hydrolysable diester linkages. These Dopa dendrimers showed a 20-fold increase in aqueous solubility and enhanced photostability in solutions over L-Dopa under identical conditions.

Li *et al.* reported the synthesis of a series of multidomain peptides (MDPs) able to self-assemble into nanofibres.[50] MDPs with the general sequence of $K_2(SLXL)_3K_2$ were prepared, where X was either serine, phenylalanine, tyrosine, or Dopa. When hydrogels were prepared by simple mixing of the Dopa-substituted MDP ($K_2(SLZL)_3K_2$) with Hank's Buffered Salt Solution (HBSS), the properties of the obtained material were similar to those of the unsubstituted peptide ($K_2(SL)_6K_2$). They then examined the possibility to induce a shear alignment of the nanofibers. The peptide $K_2(SLZL)_3K_2$ was prepared and slowly injected into the HBSS buffer solution, while dragging the pipet backward. The authors observed the formation of a string of hydrogel with unique mechanical strength, which can be easily lifted using tweezers without breaking. The examination of the string by polarized optical microscopy revealed strong birefringence along the length of the fibers, suggesting the anisotropic nature of the string, in agreement with SEM and TEM analyses, which revealed the presence of bundles of aligned nanofibres. These mechanical strength and morphology were not found in $K_2(SL)_6K_2$ (the non-containing Dopa analogue) prepared in the same way (Fig. 19). Since this difference in long-range organization could be ascribed to the aromatic side chain of Dopa, they also prepared two additional MDPs, $K_2(SLFL)_3K_2$ and $K_2(SLYL)_3K_2$, replacing Dopa with phenylalanine (F), bearing a benzyl ring but no hydroxylation, and tyrosine (Y) bearing a benzyl ring with one hydroxyl group.

When the authors prepared the gel using $K_2(SLFL)_3K_2$ and $K_2(SLYL)_3K_2$, strings were formed in both cases but did not show birefringence. In addition, these strings were not strong enough to be lifted from solution or otherwise manipulated, confirming the importance of the Dopa unit in the structure.

They also oxidised Dopa with periodate to initiate covalent cross-linking. They obtained strings that are mechanically strong enough to be manipulated and chemically resilient enough to survive transfer into media.

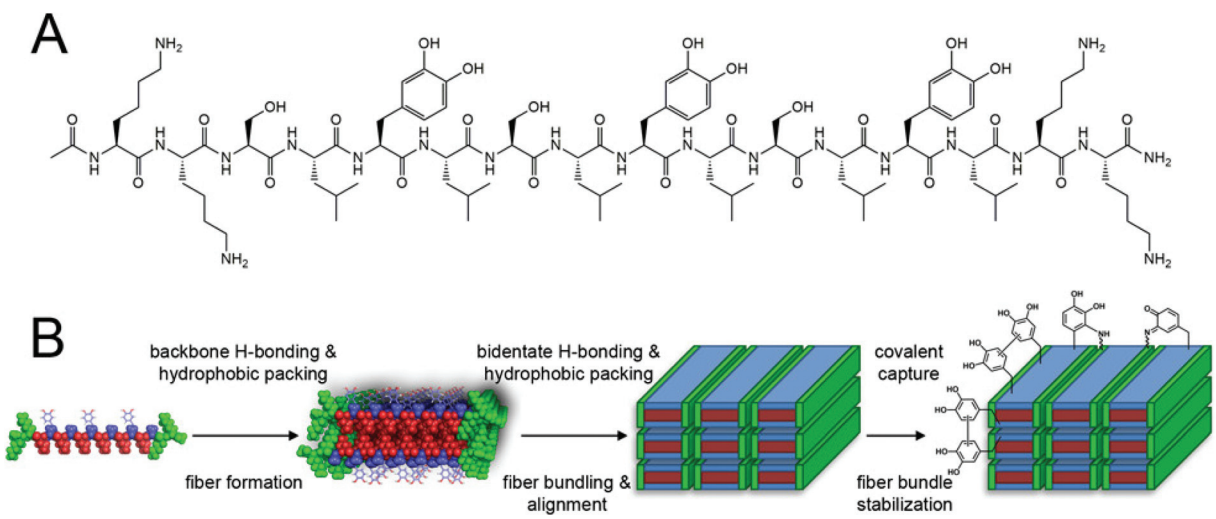

Fig. 19 (A) Chemical structure of the peptide $K_2(SLZL)_3K_2$. (B) Process of self-assembly, through fiber bundling, followed by fiber alignment and covalent capture. Upon oxidation, these groups can covalently cross-link with one another or with the amines of the lysine residues.

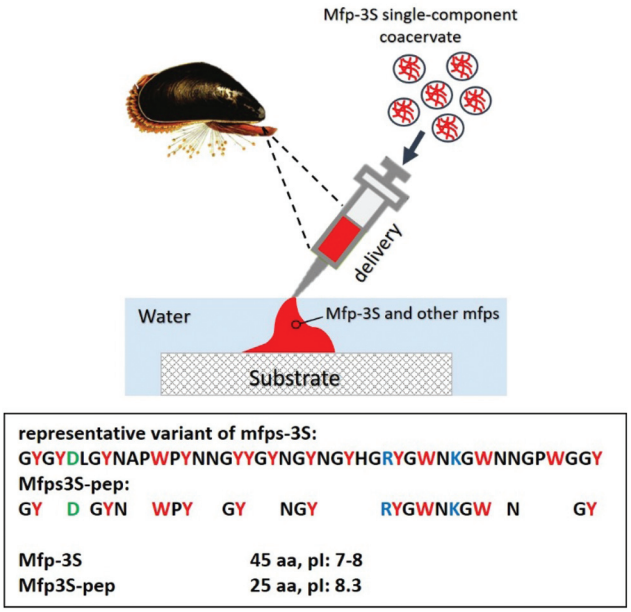

Fig. 20 (Top) Schematic illustration of mfp-3S being delivered onto a wet substrate surface as a single-component coacervate followed by its hardening into the mussel's adhesive plaque together with other mfp. (Bottom) Sequences of native mfp-3S and truncated peptide mfp3S-pep with their corresponding pI values. Letters in red, blue, and green denote aromatic, basic, and acidic amino acids, respectively.

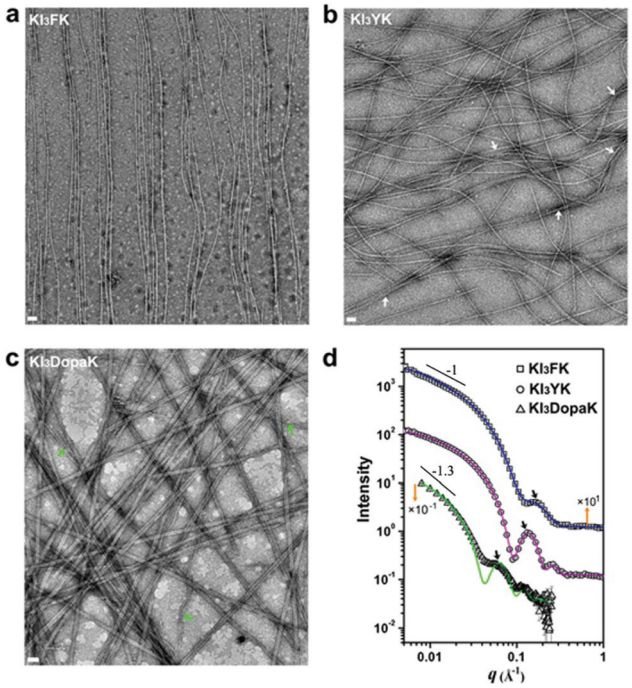

Fig. 21 Structural characterization of the self-assemblies formed by the designed bolapeptides in water (32 mM) after 1 week of incubation. (a–c) Negative-staining TEM images (scale bar, 50 nm). White arrows in (b) indicate further aggregation of thin KI_3YK assemblies, and green arrows in (c) show the presence of minor helical ribbons, as the precursor of the dominant nanotubes. (d) SANS data and model fits. Adapted with permission from ref. 52. Copyright (2021) Elsevier.

Wei *et al.* designed a peptide analogue of mfp-3 (mfp3S-pep), comprised of 25 amino acids to mimic the native protein (Fig. 20).[51] Using mushroom tyrosinase, the peptide was enzymatically modified to provide the desired level of Tyr to Dopa conversion (mfp3S-pep-Dopa). The self-coacervation of the modified and unmodified peptides was investigated over a range of pH and ionic strength values. Adsorption studies performed on hydroxyapatite (HAP) and anatase (TiO_2) confirmed that Dopa enhances the adsorption kinetics and consequently the quantity of the adsorbed peptide. HAP and TiO_2 surfaces were used for adsorption studies for their relevance in biomedical applications.

Finally, Xu *et al.* studied the dimension of the nanostructures self-assembled from short designed peptides, analysing the behaviour of peptide bolaamphiphiles (Fig. 21).[52] The structure of bolaamphiphiles favours the formation of monolayer wall nanotubes due to the interplay between the side chain structure and hydrophobicity of the central residues. The peptide KI_4K self-assembles into nanotubes with a width of ~100 nm. The three variants of KI_4K, *via* the substitution of the I residue closest to the C-terminus with aromatic amino acids (F, Y, and Dopa), reduces the nanotube diameters due to the steric hindrance of the benzene rings on the lateral packing of β-sheets. A further effect is due to the introduction of hydroxyl groups on the aromatic rings, with the nanotube diameter increasing in the order of KI_3FK, KI_3YK, and KI_3DopaK.

3. Surface coatings with L-Dopa: layers and self-assembled nanospheres

The last chapter of this review is dedicated to Dopa containing peptides that do not form materials themselves, but act as surface coatings, thus modifying the properties of the material that is treated with these peptides. We include here also the use of Dopa peptoids that mimic peptides as they are chains having an achiral α-carbon, while the chiral moiety is linked to the nitrogen.

Chen *et al.* reported the preparation of Dopa adlayers on self-assembled monolayers (SAMs) with varying end groups (–OH, $–NH_2$ and $–CF_3$).[53] The bare surface tested was gold (Fig. 22a).

The well-defined and highly ordered monolayers and the compact L-Dopa adlayers protect the substrate from corrosion, suppressing the diffusion of aggressive water and acid molecules. The authors found that the corrosion current (I_{corr}) decreases with the introduction of Dopa adlayers on $–CF_3$ and $–NH_2$ SAMs but increases with the addition of Dopa on –OH SAMs, compared with Dopa adlayers coating on the bare substrate (Fig. 22b).

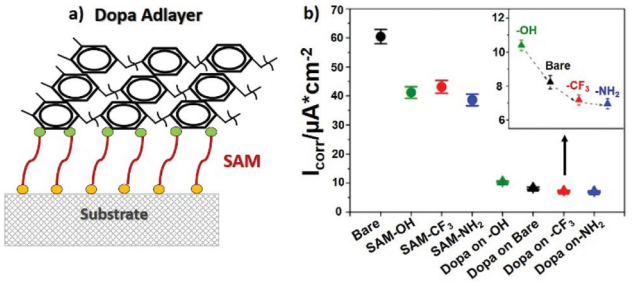

Fig. 22 (a) Formation of Dopa adlayers; (b) corrosion current obtained from potentiodynamic polarization curves for different Dopa adlayers.

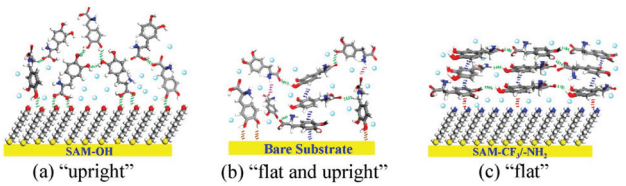

Fig. 23 Optimized preferential adsorption conformations of Dopa on (a) OH-SAMs, (b) bare substrate, and (c) CF_3- and NH_2-SAMs. Adapted with permission from ref. 53. Copyright (2019) Elsevier.

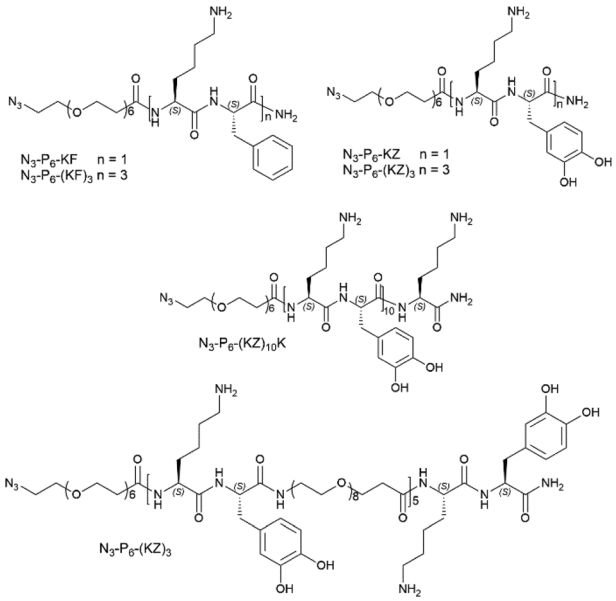

Fig. 24 Chemical structure of the synthesized peptides.

The authors correlated the corrosion resistance with the binding energy and with the molecular orientation. The binding energy values of Dopa upon OH-SAMs indicates an "upright" conformation with the carboxyl oriented perpendicular to the surface and the formation of a hydrogen bond between Dopa and OH-SAMs (Fig. 23a). In the case of the pure substrate, there are both "flat" and "upright" conformations with the phenylene ring plane lying parallel to the surface or hydroxyl group of the catechol orienting perpendicular to the surface, leading to a relatively loose and extended adlayer (Fig. 23b). The values of Dopa interacting with $-NH_2$ and $-CF_3$ SAMs suggested a "flat" conformation on both surfaces (Fig. 23c).

Another application is described by Messersmith *et al.*, who studied the adhesion of peptides of various lengths with repeating units Lys-Dopa (KZ) and Lys-Phe (KF) with polystyrene (PS) and TiO_2 (Fig. 24).[54]

On comparing (Lys-Dopa), $(Lys\text{-}Dopa)_3$, and $(Lys\text{-}Dopa)_{10}$, the authors found that the adhesion toward TiO_2 is increased from the monomer (SMFS, 120 pN) to the trimer (SMFS, 300 pN), but this remains steady for a higher number of repeating units. The TiO_2 surface is negatively charged, so it is reasonable that a major number of Lys residues results in an increase of the adhesion ability. Also, an increase in the positive charge results in better removal of the water layer from the surface to bind. In the end, in $(KZ)_3$, the repetitive sequence allows the formation of the symmetric feature Lys-Dopa-Lys, leading to more adaptable and versatile synergistic binding.

To investigate how the substitution of Dopa with Phe would affect the adhesion capability, the same oligomers, in terms of the peptide length, (Lys-Phe), $(Lys\text{-}Phe)_3$ and $(Lys\text{-}Phe)_{10}$, were synthesised and deposited on TiO_2 and polystyrene. (Lys-Phe) oligomers show remarkable adhesion capability toward polystyrene, while being slightly adhesive with TiO_2. This may be explained considering the fact that Phe interacts with the surface through cation–π and π–π interactions: a PS surface is easily bound by such molecules, while a negatively charged one is less likely to be bound, resulting in a non-detectable force for the dipeptide and a remarkably lower one for superior oligopeptides.

In another work on coating with peptides, Reches *et al.* reported a tripeptide sequence containing three elements that enable (i) self-assembly into a coating, (ii) adsorption onto any substrate and (iii) antifouling activity. To direct the assembly of the peptide, they selected two adjacent fluorinated phenylalanine residues.[55] They assumed that the aromatic interactions of this motif promote molecular recognition and direct the self-assembly of the peptide into a film. The additional carbon–fluorine bond of the fluorinated aromatic ring leads to the formation of a "Teflon-like" material that will prevent the attachment of proteins to the surface and therefore will act as an antifouling motif. The insertion of L-Dopa into the peptide sequence would act as a glue and immobilize the peptide on different substrates (Fig. 25). They compared four peptides: Dopa-Phe(4F)-Phe(4F), Dopa-Phe(F_5)-Phe(F_5), Dopa-Phe-Phe and Dopa-Phe(F_4). Overall, these results demonstrate that, to achieve antifouling activity, the peptide must contain fluorinated phenylalanine residues, which avoids the adsorption of proteins on the coated surface. The best antifouling activity was achieved with Dopa-Phe(4F)-Phe(4F).

The same group explored three variations of Dopa-Phe(4F)-Phe(4F), each with a different end group (Fig. 26).[56] This study shows that different groups at the C-terminus can lead to a

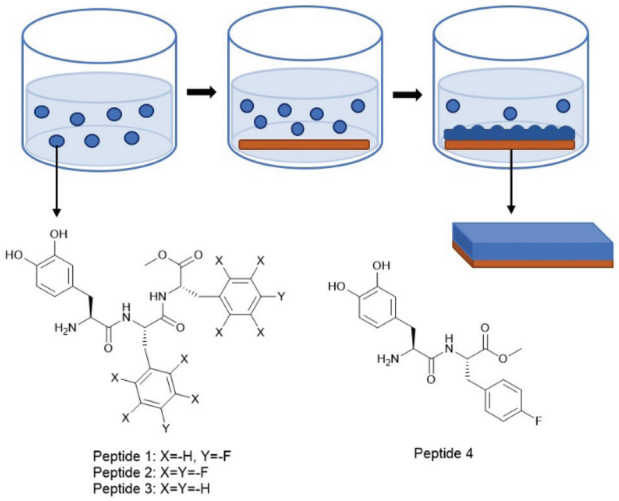

Fig. 25 (Top) Illustration showing the formation of a coating on a substrate by dip coating. (Bottom) Molecular structures of the studied peptides.

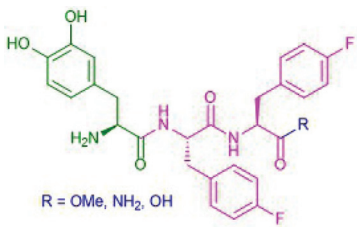

Fig. 26 The chemical structure of the peptides of R-COOMe, R-$CONH_2$, and R-COOH. Dopa is in green, the fluorinated phenylalanine is in pink, and the different ending groups are in blue.

change in the peptide assembly on the titanium surface and its adsorption process.

Peptide R-COOH had the highest adsorption, R-$CONH_2$ medium, and R-COOMe the smallest adsorption, which also corresponds to an increase in the thickness of the adsorbed layer.

The surfaces were incubated with Gram-negative and Gram-positive bacteria to assess the bacterial attachment to the surface. There was no significant difference between the peptides for the reduction of *E. coli*, while, with *S. epidermidis*, the antifouling effect was lower than with Gram-negative bacteria. This difference in bacterial adhesion (Gram positive *versus* Gram negative) might be due to the variation in surface energy.

L-Dopa was also used to mediate the immobilization of bioactive nanofibers on the titanium surface in the presence of water through catechol–titanium coordination. Ceylan *et al.* synthesized two peptide amphiphile molecules (PA) for titanium surface functionalization: lauryl-VVAGE-Dopa-Am (Dopa-PA), which is a peptide amphiphile (PA) covalently conjugated to Dopa, and another PA molecule conjugated to a heparin-binding adhesion peptide sequence, KRSR (Lauryl-VVAGKRSR-Am, KRSR-PA) (Fig. 27).[57] These molecules were tested to promote osteogenic activity. Neither Dopa-PA nor KRSR-PA formed an organized structure by themselves in solution at pH 7.4. However, upon mixing, they formed β-sheet structures within seconds, indicating β-sheet-driven nanofiber formation. The rheological analysis confirmed the formation of a weak gel with G' around 40 Pa.

The binding of the KRSR-PA/Dopa-PA nanofibers on the titanium surface was then investigated using X-ray photoelectron spectroscopy (XPS) in the presence of water after a rinsing step on the surface. They confirmed the permanent adsorption of KRSR-PA/Dopa-PA nanofibers and the formation of a peptide surface coating.

The authors also reported that osteoblastic Saos2 cells adhered in significantly greater numbers on KRSR-PA/Dopa-PA

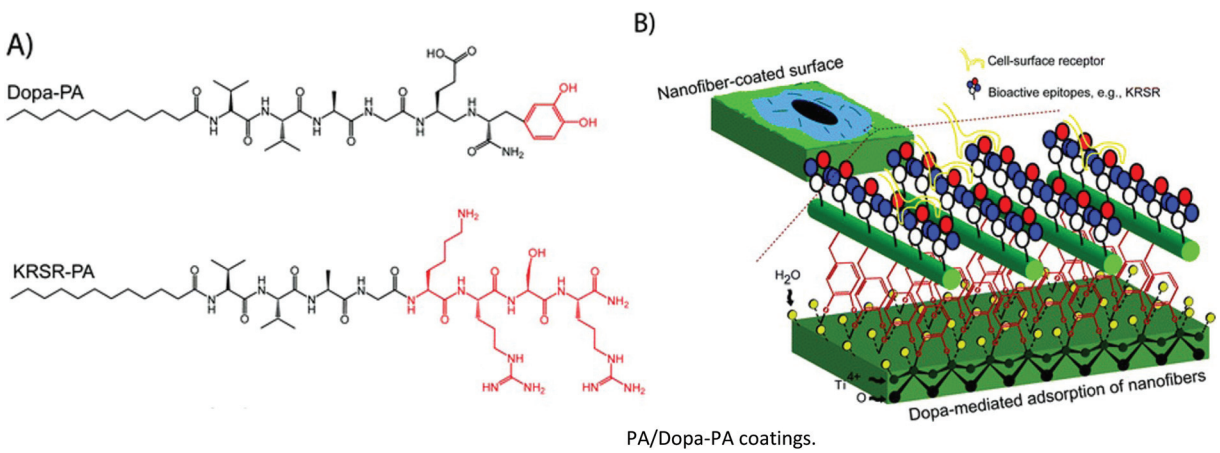

PA/Dopa-PA coatings.

Fig. 27 (A) Chemical structures of the peptide amphiphile (PA) molecules designed for functionalization of titanium surfaces. (B) Dopa-mediated immobilization of the bioactive nanofibers on the titanium surface in the presence of water is shown to occur through catechol–titanium coordination.[58] Adapted with permission from ref. 57. Copyright (2012) Royal Society of Chemistry.

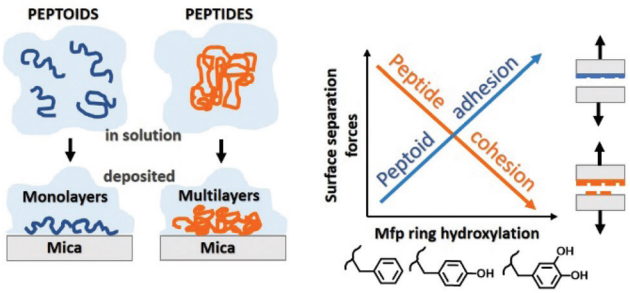

Fig. 28 Illustration of the assembly of peptoids and peptides in solution and after deposition (left). Surface separation forces in peptides and peptoids depending on the ring hydroxylation (right).

compared to the bare TiO_2 surface. The increased hydrophilicity of the decorated surface also caused a decrease in the number of human gingival fibroblasts (HGF) adhered on the surface, resulting in the designed PA coatings to selectively favour osteoblast adhesion. A selective enhancement of Saos2 cell viability was also achieved on KRSR-PA/Dopa-PA coatings.

3.1. Surface coatings with L-Dopa peptoids

The adhesive performances of mfp (mussel foot proteins) are largely due to cohesive effects. The catecholic (Dopa) and cationic (Lys, Arg) side chains work separately and in synergy to maximize both adhesion and cohesion in mfp.

On comparing Phe-, Tyr- and Dopa-peptides, Phe-peptides have the strongest cohesive forces. Cation–π interactions are the main interactions responsible for cohesion, which is limited by the steric hindrance of hydroxyl groups in the case of Tyr and Dopa.

Opposite results have been obtained by Waite *et al.* with peptoids, which are chains having an achiral α-carbon, no amide hydrogens (which prevents the formation of H bonds) and poor electron delocalization in the polyamide backbone bonds, leading to a more flexible conformation (Fig. 28).[59]

Thanks to the flexibility of their backbones, peptoids tend to deposit as a monomolecular film, while peptides deposit as multilayers and this induces an opposite trend between them. Peptoids are more hydrophobic and therefore less hydrated than Dopa-containing peptides, so the surface and molecular binding properties are largely dominated by H-bonding and cation–π interactions. Thus, for peptides, the trend in adhesion (and cohesion) is Phe > Tyr > Dopa, and for peptoids we have the opposite trend. Peptoids may be used as substitutes for peptides, maintaining the properties of the side chains, yet avoiding the complications due to the rigidity of the backbone (Fig. 29).

4. Shortcomings of the current achievements

Even though Dopa-based materials show extremely interesting properties, few precautions are needed. The oxidation of the catechol moiety should be kept under control. As previously

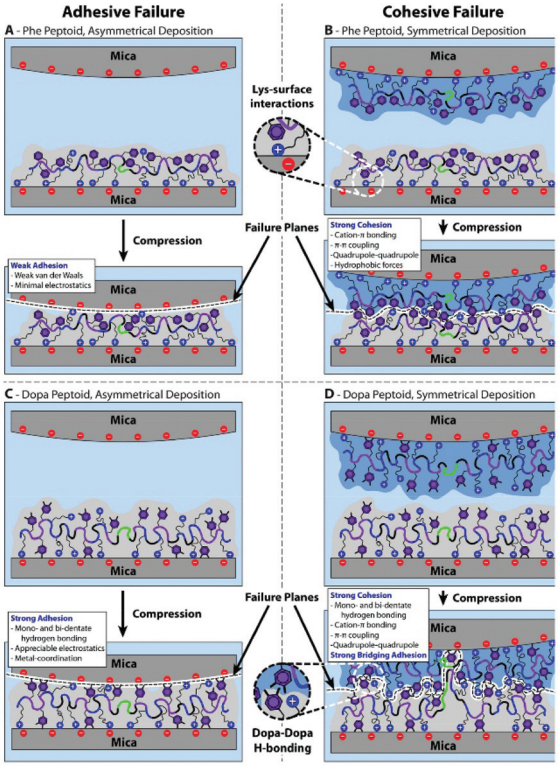

Fig. 29 Modeling peptoid adhesion *vs.* cohesion. (A) Scheme of peptoid films before and after compression for asymmetric deposition of the Phe peptoid. (B) Symmetric deposition of the Phe peptoid. (C) Asymmetric deposition of the Dopa peptoid. (D) Symmetric deposition of the Dopa peptoid. Adapted with permission from ref. 59. Copyright (2020) American Chemical Society.

discussed, quinonic and catecholic forms are able to form intermolecular H-bonds, crucial for the formation of supramolecular materials, and are useful for many of the applications already discussed, but the presence of air or basic conditions may lead to the complete oxidation of the compound. This can result in a completely different behaviour, compromising the properties of the original material.

The synthetic route of each compound may be challenging, as its complexity is increased, and the formation of the supramolecular materials should be carefully controlled to ensure reproducibility.

5. Conclusions and future perspectives

Protected Dopa and peptides containing Dopa form a group of molecules able to self-assemble into a plethora of materials holding remarkable properties ranging from gels to adhesives and nanoparticles. These peptides may also functionalize the surfaces of materials to modify their properties. These results are some examples of applications of materials obtained by the self-assembly of Dopa derivatives. These molecules alone or in addition to other functional materials may be applied to

the production of smart materials that may be used also for surface functionalization. These coatings present high stability to adhere to all types of substrates and can be useful in different biomedical applications.

The capability of Dopa to form supramolecular materials is due to the presence of multiple interacting sites present on it that make it a multifunctional building block. The possibility to form hydrogen bonds and the presence of the aromatic ring allow L-Dopa molecules to interact through a series of non-covalent interactions. The additional presence of the catechol moiety has implications in the self-assembly process of Dopa itself and with other substrates.

In this review, we have collected a wide variety of examples that have been classified according to the peptide size. It is remarkable to see that even protected Dopa can form several different materials, by simply changing the protecting groups, the solvent and the trigger. The versatility of more complex peptides is even higher. We hope that this review will spur the community of chemists to make further efforts in the study of Dopa-based materials.

Author contributions

Conceptualization: DG and CT; funding acquisition: CT; investigation: DG and PR; writing – original draft: DG, PR and CT; writing – review & editing: DG, PR and CT.

Conflicts of interest

There are no conflicts to declare.

Notes and references

1 D. A. Robb, *Tyrosinase*, CRC Press, 2018.
2 M. T. Varela, M. Ferrarini, V. G. Mercaldi, B. da S. Sufi, G. Padovani, L. I. S. Nazato and J. P. S. Fernandes, *Bioorg. Chem.*, 2020, **103**, 104108.
3 K. Min, D. H. Park and Y. J. Yoo, *J. Biotechnol.*, 2010, **146**, 40–44.
4 E. Waser and M. Lewandowski, *Helv. Chim. Acta*, 1921, **4**, 657–666.
5 T. Shimidzu, T. Iyoda and N. Kanda, *J. Chem. Soc., Chem. Commun.*, 1981, 1206–1207.
6 T. Ooi, M. Kameda, H. Tannai and K. Maruoka, *Tetrahedron Lett.*, 2000, **41**, 8339–8342.
7 I. A. Sayyed and A. Sudalai, *Tetrahedron: Asymmetry*, 2004, **15**, 3111–3116.
8 R. H. Valdés, L. Puzer, M. Gomes, C. E. S. J. Marques, D. A. G. Aranda, M. L. Bastos, A. L. Gemal and O. A. C. Antunes, *Catal. Commun.*, 2004, **5**, 631–634.
9 D. Magdziak, A. A. Rodriguez, R. W. Van De Water and T. R. R. Pettus, *Org. Lett.*, 2002, **4**, 285–288.
10 R. Bernini, M. Barontini, F. Crisante, M. C. Ginnasi and R. Saladino, *Tetrahedron Lett.*, 2009, **50**, 6519–6521.
11 M. D'Ischia, A. Napolitano, V. Ball, C. T. Chen and M. J. Buehler, *Acc. Chem. Res.*, 2014, **47**, 3541–3550.
12 J. H. Waite, *Int. J. Adhes. Adhes.*, 1987, **7**, 9–14.
13 S. A. Mian and Y. Khan, *J. Chem.*, 2017, **2017**, 1–6.
14 J. H. Waite, *J. Exp. Biol.*, 2017, **220**, 517–530.
15 S. Barbara, *Biochemistry*, 2002, **1180**, 1172–1180.
16 J. H. Waite and M. L. Tanzer, *Top. Catal.*, 1980, **96**, 1554–1561.
17 B. P. Lee, P. B. Messersmith, J. N. Israelachvili and J. H. Waite, *Annu. Rev. Mater. Res.*, 2011, **41**, 99–132.
18 H. Zhao, C. Sun, R. J. Stewart and J. H. Waite, *J. Biol. Chem.*, 2005, **280**, 42938–42944.
19 J. H. Waite, *Integr. Comp. Biol.*, 2002, **42**, 1172–1180.
20 W. Zhang, R. Wang, Z. M. Sun, X. Zhu, Q. Zhao, T. Zhang, A. Cholewinski, F. Yang, B. Zhao, R. Pinnaratip, P. K. Forooshani and B. P. Lee, *Chem. Soc. Rev.*, 2020, **49**, 433–464.
21 N. Pandey, L. F. Soto-Garcia, J. Liao, P. Zimmern, K. T. Nguyen and Y. Hong, *Biomater. Sci.*, 2020, **8**, 1240–1255.
22 W. Y. Quan, Z. Hu, H. Z. Liu, Q. Q. Ouyang, D. Y. Zhang, S. D. Li, P. W. Li and Z. M. Yang, *Molecules*, 2019, **24**, 1–27.
23 L. Li, W. Smitthipong and H. Zeng, *Polym. Chem.*, 2015, **6**, 353–358.
24 Q. Guo, J. Chen, J. Wang, H. Zeng and J. Yu, *Nanoscale*, 2020, **12**, 1307–1324.
25 P. K. Forooshani and B. P. Lee, *J. Polym. Sci., Part A: Polym. Chem.*, 2017, **55**, 9–33.
26 I. Manolakis and U. Azhar, *Coatings*, 2019, **10**(7), 653.
27 B. K. Ahn, S. Das, R. Linstadt, Y. Kaufman, N. R. Martinez-Rodriguez, R. Mirshafian, E. Kesselman, Y. Talmon, B. H. Lipshutz, J. N. Israelachvili and J. H. Waite, *Nat. Commun.*, 2015, **6**, 1–7.
28 H. T. Peng and P. N. Shek, *Expert Rev. Med. Devices*, 2010, **7**, 639–659.
29 M. De Loos, B. L. Feringa and J. H. Van Esch, *Eur. J. Org. Chem.*, 2005, 3615–3631.
30 J. Wang, K. Liu, R. Xing and X. Yan, *Chem. Soc. Rev.*, 2016, **45**, 5589–5604.
31 E. R. Draper and D. J. Adams, *Chem*, 2017, **3**, 390.
32 X. Du, J. Zhou, J. Shi and B. Xu, *Chem. Rev.*, 2015, **115**, 13165–13307.
33 C. Tomasini and N. Castellucci, *Chem. Soc. Rev.*, 2013, **42**, 156–172.
34 A. Saha, S. Bolisetty, S. Handschin and R. Mezzenga, *Soft Matter*, 2013, **9**, 10239.
35 G. Fichman, T. Guterman, J. Damron, L. Adler-Abramovich, J. Schmidt, E. Kesselman, L. J. W. Shimon, A. Ramamoorthy, Y. Talmon and E. Gazit, *Sci. Adv.*, 2016, **2**, 1–11.
36 K. A. Houton, K. L. Morris, L. Chen, M. Schmidtmann, J. T. A. Jones, L. C. Serpell, G. O. Lloyd and D. J. Adams, *Langmuir*, 2012, **28**, 9797–9806.
37 G. Fichman, T. Guterman, L. Adler-abramovich and E. Gazit, *CrystEngComm*, 2015, **17**, 8105–8112.
38 D. Giuri, L. Jurković, S. Fermani, D. Kralj, G. Falini and C. Tomasini, *ACS Appl. Bio Mater.*, 2019, **2**, 5819–5828.
39 C. Lee, S. H. Kim, J. H. Jang and S. Y. Lee, *Sci. Rep.*, 2017, **7**, 1–11.

40 D. Giuri, K. A. Jacob, P. Ravarino and C. Tomasini, *Eur. J. Org. Chem.*, 2020, 7144–7150.
41 N. Zanna, D. Iaculli and C. Tomasini, *Org. Biomol. Chem.*, 2017, **15**, 5797–5804.
42 C. Tomasini and N. Zanna, *Biopolymers*, 2017, **108**, 1–14.
43 D. Giuri, N. Zanna and C. Tomasini, *Gels*, 2019, **5**, 27.
44 G. Fichman, L. Adler-Abramovich, S. Manohar, I. Mironi-Harpaz, T. Guterman, D. Seliktar, P. B. Messersmith and E. Gazit, *ACS Nano*, 2014, **8**, 7220–7228.
45 Y. Li, M. Qin, Y. Cao and W. Wang, *Sci. China: Phys., Mech. Astron.*, 2014, **57**, 849–858.
46 G. Fichman, T. Guterman, L. Adler-Abramovich and E. Gazit, *Nanomaterials*, 2014, **4**, 726–740.
47 K. L. Veldkamp, P. J. Tubergen, M. A. Swartz, J. T. DeVries and C. D. Tatko, *Inorg. Chim. Acta*, 2017, **461**, 120–126.
48 M. R. Eftink, L. R. A. Selvidge, P. R. Callis and A. A. Rehms, *J. Phys. Chem.*, 1990, **94**, 3469–3479.
49 S. Tang, L. J. Martinez, A. Sharma and M. Chai, *Org. Lett.*, 2006, **8**, 4421–4424.
50 I. C. Li and J. D. Hartgerink, *J. Am. Chem. Soc.*, 2017, **139**, 8044–8050.
51 W. Wei, L. Petrone, Y. Tan, H. Cai, J. N. Israelachvili, A. Miserez and J. H. Waite, *Adv. Funct. Mater.*, 2016, **26**, 3496–3507.
52 Y. Zhao, X. Hu, L. Zhang, D. Wang, S. M. King, S. E. Rogers, J. Wang, J. R. Lu and H. Xu, *J. Colloid Interface Sci.*, 2021, **583**, 553–562.
53 T. Chen, M. Yang, H. Yang, R. Wang, S. Wang, H. Zhang, X. Zhang, Z. Zhao and J. Wang, *J. Ind. Eng. Chem.*, 2019, **69**, 179–186.
54 Y. Li, J. Cheng, P. Delparastan, H. Wang, S. J. Sigg, K. G. DeFrates, Y. Cao and P. B. Messersmith, *Nat. Commun.*, 2020, **11**, 1–8.
55 S. Maity, S. Nir, T. Zada and M. Reches, *Chem. Commun.*, 2014, **50**, 11154–11157.
56 A. Dolid and M. Reches, *J. Pept. Sci.*, 2019, **25**, e3212.
57 H. Ceylan, S. Kocabey, A. B. Tekinay and M. O. Guler, *Soft Matter*, 2012, **8**, 3929–3937.
58 T. H. Anderson, J. Yu, A. Estrada, M. U. Hammer, J. H. Waite and J. N. Israelachvili, *Adv. Funct. Mater.*, 2010, **20**, 4196–4205.
59 W. R. Wonderly, T. R. Cristiani, K. C. Cunha, G. D. Degen, J. E. Shea and J. H. Waite, *Macromolecules*, 2020, **53**, 6767–6779.
60 J. X. Xu, Z. Zhou, B. Wu and B. F. He, Enzymatic formation of a novel cell-adhesive hydrogel based on small peptides with a laterally grafted l-3,4-dihydroxyphenylalanine group, *Nanoscale*, 2014, **6**(3), 1277–1280.